Analyst

A review of the effects of FSCV and microdialysis measurements on dopamine release in the surrounding tissue

Journal:	*Analyst*
Manuscript ID:	AN-MRV-11-2014-002065.R2
Article Type:	Minireview
Date Submitted by the Author:	20-Mar-2015
Complete List of Authors:	Jaquins-Gerstl, Andrea; University of Pittsburgh, Chemistry Michael, A; University of Pittsburgh, Department of Chemistry

A review of the effects of FSCV and microdialysis measurements on dopamine release in the surrounding tissue

Andrea Jaquins-Gerstl and Adrian C. Michael*
Department of Chemistry, University of Pittsburgh, Pittsburgh, PA

KEYWORDS: *Microdialysis, Voltammetry, Dopamine, Dexamethasone, Fast Scan Cyclic Voltammetry, Immunohistochemistry, Penetration Injury*

Abstract

Microdialysis is commonly used in neuroscience to obtain information about the concentration of substances, including neurotransmitters such as dopamine (DA), in the extracellular space (ECS) of the brain. Measuring DA concentrations in the ECS with *in vivo* microdialysis and/or voltammetry is a mainstay of investigations into both normal and pathological function of central DA systems. Although both techniques are instrumental in understanding brain chemistry each has its shortcomings. The objective of this review is to characterize some of the tissue and DA differences associated with each technique *in vivo.* Much of this work will focus on immunohistochemical and microelectrode measurements of DA in the tissue next to the microdialysis probe and mitigating the response to the damage caused by probe implantation.

1. Introduction

Monitoring neurotransmitters in the ECS of living brain tissue has yielded seminal contributions to our understanding of brain function and the pathology associated with brain disorders, diseases, and injuries. Nevertheless, many aspects of brain function and pathology remain to be fully understood, so the pursuit of enhanced capabilities for *in vivo* chemical monitoring remains of great interest. Microdialysis has been a workhorse and a gold standard in the field for many years.[1-11] A major driving force behind the widespread use of microdialysis is

its broad scope: brain dialysate samples contain a plethora of interesting small molecules, including neurotransmitters, amino acids, neuropeptides, and more (Table 1 provides a partial list). Many of these are not accessible by other means. For example, electrochemical methods, such as fast-scan cyclic voltammetry (FSCV), present an alternative approach to *in vivo* neurochemical measurements but require the target molecule to be electroactive and distinct from interferents: most in Table 1 are not.

Despite the widespread use of microdialysis, several very early studies in the field raised concerns over the impact of the probes on brain tissues. The probes, which typically have diameters approximately 300 μm, are substantially larger than the cells (neurons and glia, 5-100 μm), myelinated fiber bundles (0.2-2 μm), blood capillaries and vessels (8-10 μm and ~1 mm) of the brain parenchyma and their spacing.[12] This raised the concern that implanting the probes might damage the tissue. Indeed, some early studies suggested that this might be the case. A very early study in the field showed that the dialysate concentration of DA and its sensitivity to tetrodotoxin (TTx) varies substantially over the 24hr following implantation of the probe into the striatum of the rat.[9] Other studies have also documented instability in DA measurements over both longer and shorter time intervals following probe implantation.[9, 13-17] Histochemical studies with both light and electron microscopy showed that the tissues near microdialysis probe tracks exhibit signs of traumatic injury, thus it seems plausible that the instability in the dopamine measurements might be attributable to the damage that occurs when the probes are implanted.[18, 19] Traumatic injury of the brain sets off a cascade of events, collectively known as the foreign body response (FBR), that occur in sequential stages lasting hours, days, and weeks after the injury takes place.

The idea that microdialysis results depend upon the time interval following probe implantation is widely, although perhaps tacitly, acknowledged in the field. All microdialysis protocols include a consistent wait time after the probe is implanted before experiments are initiated.[19-21] Most microdialysis protocols are acute, i.e. the experiments are performed within a well-defined time window, usually less than 24 hours and then the experiment is terminated. Chronic, longitudinal microdialysis studies in the brain are not routinely performed.

By the end of the 1990s, however, there was no clear evidence establishing that the dependence of microdialysis results on the wait time after the probe implantation was actually caused by the penetration injury or the FBR.[22-24] We became interested in this matter when we observed that electrically evoked DA responses measured by FSCV were altered, sometimes dramatically, if a microdialysis probe was implanted nearby the voltammetric carbon fiber microelectrode, Fig. 1.[25] This was the first, and remains the only, clear documentation that implanting a microdialysis probe changes the DA activity in the brain tissue next to the probe. More important, is that "voltammetry next to the probe" has started to prove itself as a very useful quantitative tool for guiding our efforts towards mitigating the penetration injury and the FBR via the addition of anti-inflammatory and anti-oxidant drugs to the microdialysis perfusion fluid: this is called retrodialysis. To assess the efficacy of our retrodialysis mitigation strategy, we have been using immunohistochemistry to examine the tissue near the probe tracks by fluorescence microscopy in addition to voltammetric measurements of DA in the tissue next to the probe. Herein, we review our efforts to date.

1. The DA gradient near microdialysis probes

As mentioned above, FSCV is a complimentary technique to microdialysis that permits *in vivo* measurements of several electroactive substances, including DA. The measurements are performed with an implanted carbon fiber microelectrode, a device with dimensions that are far smaller than those of a microdialysis probes: the electrodes we use have a diameter of 7 μm and an active length that we vary, depending on the experiment, between 100 and 400 μm. We have attempted to examine the tissue damage caused by these electrodes but the damage is so minimal it is very difficult to observe. The track of a carbon fiber electrode is usually invisible at the level of light microscopy. We have used electron microscopy to view the probe track but only with great difficulty (Fig. 2).[26] Whatever amount of tissue damage the microelectrodes cause is clearly minimal in comparison to that caused by microdialysis probes, which is easily visualized by light microscopy.

FSCV in conjunction with carbon fiber microelectrodes has been used extensively to measure rapid fluctuations in extracellular DA concentrations during electrical stimulation of DA axons. Depending on the exact stimulus conditions, FSCV detects evoked increases in DA in the micromolar concentration range lasting for a few milliseconds to several seconds (see Fig. 3 for 1 second examples) depending on the stimulus length.[27] The DA concentration rapidly returns to baseline levels after the stimulus ends due to the actions of the DA transporter, the transmembrane protein that removes DA molecules from the extracellular space and returns them to DA terminals, where they are repackaged into synaptic vesicles and reused at a later time.[28] However, we noticed that if a microdialysis probe is implanted nearby a carbon fiber microelectrode, the amplitude of the evoked DA response decreases in a manner that depends upon the distance of separation between the probe and the carbon fiber (Fig. 4).[29] If the probe is

implanted ~1 mm from the carbon fiber, then there is no significant loss in response amplitude. However, if the probe is positioned 200 μm from the fiber there is ~90% loss in amplitude. In a set of experiments where we glued the carbon fiber onto the outer surface of the microdialysis probe, to achieve a zero separation distance, then the response amplitude was lost completely (Fig. 4).[29] These observations revealed, for the first time that the implantation of a microdialysis probe leads to a gradient of disrupted DA activity in the tissues surrounding the probe track. The response amplitude could be partially restored by treating the animals with nomifensine, a DA uptake inhibitor, and the post-nomifensine response also exhibited a gradient in amplitude (Fig. 5). The gradient observations summarized here were made 4 hrs after implanting the probe. When we extended the interval after probe implantation to 16 hr, we found even less evoked DA: thus, our results added to the available evidence of instability in DA responses as a function of the post-implant interval.[17]

Obviously, the loss in the amplitude of the evoked responses caused by the implantation of the microdialysis probe is a sign that the DA activity near the probe is disrupted from its normal state. Although the amplitude of the evoked responses was smaller nearest to the probe, it does not appear that the probes simply destroyed the DA terminals. If this were the case, then it is very doubtful that we would have been able to partially reinstate the responses with nomifensine, an uptake inhibitor. In fact, on a proportional basis, the effects of nomifensine were largest nearest the probe. This implies that the DA uptake mechanism remains active near the probe, even though DA release had been suppressed. A key point here is that the DA transporter is only expressed by DA terminals: no other cells or axon terminals within the rat striatum carry this protein. So, if the DA transporter is present near the probe, then so too are the DA terminals (presumably surviving the implantation).

Hence, a major implication stemming from the observations of the DA gradient in the tissue next to the probe is that DA terminals near the microdialysis probe survive the tissue damaging effects of the probe implantation. This has motivated our subsequent efforts to promote the survival and stability of DA terminals via the retrodialysis of anti-inflammatory and anti-oxidant drugs, as explained in sections 2 and 3 of this review.

The other major implication of our findings is that microdialysis samples of DA are recovered from the brain tissue next to the probe wherein DA activity is disrupted from its normal state. As mentioned above, signs that the probes cause trauma were first reported in the literature in 1980s, so this implication comes as no great surprise.[9, 30] Nevertheless, the impact of the trauma and ensuing foreign body response on neurochemical results has not been explored deeply. One very well known microdialysis observation is that DA uptake inhibitors, including nomifensine, dramatically increase dialysate DA levels, in some cases as much as 320%.[31] In contrast, this observation has been quite difficult to reproduce by FSCV. We routinely conduct experiments involving nomifensine administration: nomifensine very clearly and consistently alters the DA responses we measure with FSCV during electrical stimulation. But, we have never observed the same magnitude of increase in DA levels. In the absence of electrical stimulation FSCV produced a 2 fold increase after administration of nomifensine (2 ± 1.2 μM) at an electrode 220-250 μm from the probe compared to the microdialysis sample which increased 10-fold over pre-nomifensine drug level (144.1± 18.9 nM).[29] The FSCV response was only measurable in the case where the carbon fiber microelectrode was positioned close to a microdialysis probe, where, as we explained above, the affects of the drug appear to be magnified.[32] Some of this difference may be attributed to the different temporal resolution between these two techniques. Although we have pointed out in several papers that microdialysis

and FSCV lead to different results for DA, this is not necessarily the case if the carbon fiber electrode is close to the probe.[25, 32] In that case, the microelectrode and the microdialysis probe are monitoring the same tissues. Overall, these observations show that it is necessary when doing microdialysis to keep in mind that the tissue near the probes behaves somewhat differently from normal, uninjured tissue that has not been penetrated with a probe.

This idea that DA within the tissue next to microdialysis probes behaves somewhat differently than that of non-implanted tissue offers a plausible explanation for some differences we have encountered between DA results obtained by microdialysis and FSCV (in the absence of microdialysis probes). For example, the basal concentration of DA reported in microdialysis studies is typically around 10 nM, a DA concentration that is well below the detection limits typically reported for FSCV.[29, 33] But, in a series of experiments involving the intrastriatal infusion of kynurenate, a broad-spectrum antagonist of the ionotropic glutamate receptors, we observed robust decreases in DA from its resting levels (Fig. 6). [32] The decreases appeared to be of micromolar magnitudes, which would be impossible if the basal concentration were, as suggested by microdialysis, only 10 nM. Again, this observation indicates that the basal concentration in the tissue near the probe might be lower than that in non-penetrated tissues.

The results of our studies with kynurenate remain, we acknowledge, quite controversial. Not only is our estimate of the basal DA concentration dramatically different from the accepted value from microdialysis, the basal concentration exhibits some unusual behaviors. According to our findings, the kynurenate-induced decrease in basal DA concentration is sensitive to nomifensine, the DA uptake inhibitor, and insensitive to TTx (Fig. 7).[32] This is classic profile of the so-called reverse transport mode of release, i.e. the release of DA via the reversal of the DA transporter. According to microdialysis, reverse transport does not occur except when animals

receive amphetamine or amphetamine-like drugs. The full implications of our conclusion that reverse transport occurs normally, i.e. without amphetamine administration, remain to be elucidated.[34] Nevertheless, this is yet another example where microdialysis and FSCV lead to rather different conclusions about DA and DA function.

2. Immunohistology of probe implantation and mitigating damage

Another important factor involved in implanting these two devices in living brain tissue is the brain vasculature. The distance separating blood vessels in the rat striatum is approximately 50 μm, (considerably less than the diameter of microdialysis probes), thus, it is very reasonable that blood vessels are affected by probe implantation. Blood vessels, which carry red blood cells responsible for oxygen release, are in direct communication with neurons. In the case of DA, oxygen delivery to neurons through blood vessels is required to allow tyrosine hydroxylase to convert tyrosine to DOPA, which can then be converted to DA. This DA is packaged and available for release upon stimulation.[35] A break-down in oxygen delivery would be detrimental in DA release, uptake, and detection.

Damaged blood vessels may also lead to the breakdown or increased permeability of the blood brain barrier (BBB). The placement of any device in the *in vivo* environment requires injection, insertion or surgical implantation, all of which damages the target tissues. The physical dimensions of the microdialysis probes and carbon fiber electrodes are quite different from one another. Penetration trauma from these two techniques can be diminished simply by decreasing the size of the implanted device. Carbon fibers have, approximately, a 30-fold smaller diameter, a 10-fold shorter active length, and occupy a roughly 10,000-fold smaller total volume than microdialysis probes. The differences in the physical dimensions of these two devices lead to

differences in the extent of traumatic brain injury which they inflict. Evidence of damage to the brain tissue surrounding implanted microdialysis probes demonstrate that these devices are too large to use *in vivo* without disrupting the normal anatomy of the tissue. Drew and coworkers reported significantly decreased trauma in hibernating animals following brain penetration when compare to euthermic animals, suggesting that a contributing factor in traumatic brain injury could be a disruption in blood flow.[18, 19] Studies from our group have demonstrated that disrupted blood flow through capillaries in the vicinity of microdialysis probes after 4 hours of implantation compromises the integrity of the BBB. Others have also demonstrated that employment of microdialysis probe disrupts vasculature compromising the BBB. There is a dramatic consequence once the blood-brain barrier is opened. Continuums of wound healing processes occur due to the presence of the probe and the penetration injury leading to a FBR. Often data obtained from this type of response can be misleading. The precise mechanism by which the foreign body response limits neural devices remains unclear.

There are many consequences associated with the penetration of any device into brain tissue; this is especially true when dealing with the BBB.[36] In our hands we have experienced tissue abnormalities during probe insertions. We found carbi-DOPA, a drug molecule that normally does not cross the BBB, in brain dialysates, Fig. 8.[37] This is evidence that the probes open the BBB. We also found that fluorescent nanobeads used to represent blood flow spill out of blood vessels near microdialysis probes, but not elsewhere in the brain, providing direct evidence that the BBB is opened, as shown in Fig.9. [38] In this study green fluorescent nanobeads were perfused through the bloodstream and blood vessels were labeled with anti-PECAM (PECAM is a protein, platelet endothelial cell adhesion molecule) post mortem. We observed attenuation of blood flow to the probe site (Fig. 9B-D), confirming a localized ischemic event. Endothelial debris forming a halo of

diffuse anti-PECAM labeling surrounding the tracks was clearly evident. Another hallmark of the brain-tissue reaction to implanted probes is the formation of hypertrophic astrocytes surrounding the implantation site. Following injury, astrocytic processes form a scar-like layer surrounding the implanted device. These astrocytes form a capsule to isolate or wall off the implant from the rest of the brain tissue in a process known as astrogliosis.

Studies from our lab, Fig. 10a, have shown that after 24-h implantations, microdialysis probe tracks are surrounded by hyperplasic and hypertrophic glia and the tracks are in the initial stages of being engulfed by gliosis.[38] Three quarters of the circumference of the probe track is surrounded by glial processes as shown in Fig. 10a. In one case, Fig. 10b, a glial fibrillary acidic protein (GFAP) immunoreactive cell extends a distance of 300 μm towards the probe track, which indicates a chemotaxic mode of communication between the injury site and nearby glia was observed. These long extensions are completely absent in images of control tissues (tissue that did not receive a microdialysis probe implant) and in tissues that contained carbon fiber microelectrodes. In general, evidence shows that the smaller devices are better in part because they are less traumatic to the tissue. We recognize that glial processes are inserting themselves into the space between the probe and neighboring DA and glutamate terminals and interfering with the ability to detect the neurotransmitters.[39] This process of gliosis will eventually isolate the probe. [40]

One of the underlying concepts in our work is that manipulations of this abnormal layer can be a clear route to refining and enhancing microdialysis as a neurochemical tool. Since existing probes are already as small as practicably possible without using a microfabrication process, our strategy is to diminish the injury by mitigating the tissue response. This will allow diffusional communication between the probe and the surrounding tissue, so that dialysate concentrations provide an improved index of *in vivo* concentrations. As such, successes have been achieved in the

control of inflammation and gliosis in the context of neuroprosthetic devices. Devices, such as microfabricated silicon electrodes, have been coated with polymer layers that release anti-inflammatory agents.[41-44] A major advantage of microdialysis is that it permits the direct delivery of agents to the brain: this has been called retrodialysis and reverse dialysis in the literature.[9, 45] Rather than relying on controlled-release polymers for agent delivery, during microdialysis the agent of interest is added to the perfusion fluid with excellent control over the concentration, delivery time, and delivery duration. We investigated dexamethasone (DXM), a powerful steroidal anti-inflammatory drug that proved successful in reducing the glial response to many neuroprosthetics.[42, 44, 46]

DXM is a potent suppressant of the wound healing response and is used to treat many inflammatory responses. Delivery of DXM has proven therapeutically useful in central nervous system disorders.[47] DXM has also been used to inhibit the immune response to microdialysis probes implanted subcutaneously. [48] As far as we know, we were the first to investigate the impact of DXM on tissue abnormalities associated with microdialysis probes in the brain. We performed microdialysis in the rat brain for 5 days with and without DXM in the perfusion fluid. [49] On the first and fourth day of the perfusion DA no-net-flux measurements were performed, and at the end of the perfusion brain tissues were sectioned, stained, and examined by fluorescence microscopy to assess gliosis and ischemia. Microdialysis probes induce gliosis around the probe track. GFAP immunofluorescence revealed profound gliosis at the tracks of microdialysis probes after 5 day perfusions in the rat brain (Fig. 10c). Glia surrounding the probe tracks exhibit enlarged cell bodies and thickened and elongated processes (Fig. 10d, e, and f). The images in Fig.10 extend our previous report that gliosis is evident after 24 h perfusions. After 5 days of implantation, microdialysis probe tracks become fully engulfed by GFAP-labeled

cells (Fig. 10g). Retrodialysis of DXM dramatically inhibits probe-induced gliosis (Fig. 10h). Probe-implanted tissues showed more GFAP labeling than non-implanted control tissues however, they showed far less GFAP labeling in the presence of DXM. Without DXM (Fig. 10g), the track is surrounded by a continuous glial barrier that maintains the shape of the probe track. Proteoglycan secretions of activated glia can be attributed to the rigidity of the glial barrier.[50] Because retrodialysis of DXM prevented the formation of a glial barrier, the tracks typically did not maintain their fully open and circular shape. The remaining gliosis after DXM retrodialysis is asymmetric and, in this example, is almost nonexistent around approximately half the circumference of the track. These findings show that DXM is highly effective at suppressing gliosis.

Another feature in this study was that DXM prevented ischemia; we were not surprised to notice extensive ischemia 5 days after the implantation of probes that were not perfused with DXM. The retrodialysis of DXM inhibited this ischemia: bead-laden vessels appeared essentially normal after 5 days of perfusion with DXM. We speculated that the migration of glial cells to the probe track eventually interferes with blood flow and re-establishes the blockade of vessels. Thus, DXM, in addition to inhibiting gliosis, also prevented ischemia at the probe tracks. Because the impact of DXM on gliosis and ischemia is apparent, our findings clearly prove that DXM alters the state of the tissue near the probes and we became interested in knowing if this, in turn, alters the outcome of microdialysis sampling. To investigate this, we measured no-net-flux curves for DA. Microdialysis extraction curves were obtained by perfusing the probe with various concentrations of the analyte of interest, here DA, and measuring its concentration at the probe outlet. The results are presented in the form of a concentration-differences plot, where the difference between the inlet concentration, C_{in}, and outlet concentration, C_{out} are plotted against

the inlet concentration, i.e. a plot of C_{in}-C_{out} v. C_{in}. The resulting extraction curve is expressed as:

$$C_{in} - C_{out} = E \cdot C_{in} - R \cdot C_{ext} \qquad \text{(Eq. 1)}$$

where R is the recovery factor, C_{ext} is the concentration in the medium external to the probe, and E (the slope of the extraction curve) is the extraction factor.

Retrodialysis of DXM clearly alters DA extraction curves measured in the rat striatum both 1 day (Fig. 11a) and 4 days (Fig. 11b) after probe implantation. Whereas DA extraction curves are linear in the absence of DXM, they become non-linear in the presence of DXM. Normally DA extraction curves are linear, and to our knowledge, these are the first non-linear microdialysis extraction curves observed for DA. Smith and Justice demonstrated many years ago that uptake inhibitors decrease DA's extraction slope.[33] However, it was unexpected that DA extraction curves were linear because DA uptake exhibits nonlinear Michaelis-Menton kinetics. According to Michaelis-Menton kinetics, when the concentration of DA rises above the K_M value (near 200 nM) of the DA transporter, the transporter becomes saturated and DA inhibits its own uptake; note that DA uptake is mediated by the DA transporter. We attributed the non-linear extraction curves to the Michaelis-Menton kinetics of DA uptake in the tissue next to the microdialysis probes. This implies that DXM preserved DAergic activity near the probe track. The results suggested that by opening the glial barrier DXM promoted the diffusion of DA to the transporter, enabling DA to more readily reach the concentrations necessary to saturate the transporter. Alternatively, DXM might promote the survival of DA terminals near the probe, so DA does not have to diffuse as far as usual to reach the transporter. This is an encouraging sign that DXM may have inhibited the adventitious destruction of DAergic elements

of the tissue by the reactive glia. Results from this study support that retrodialysis of DXM inhibits probe-induced gliosis and ischemia and preserves DAergic function in the tissue next to the probe tissue at 5 days. Thus, these results open the way towards a productive avenue of research into pharmaceutical strategies to address the as-yet unresolved issues in microdialysis stemming from the phenomenon of probe-induced penetration injury.

3. Microelectrode measurements in tissue next to a microdialysis probe

Motivated by previously mentioned studies, where DXM exhibited a profound ability to restore blood flow and suppress gliosis. We hypothesized the possibility that the DA results are mainly dependent on the state of the brain tissue immediately adjacent to the probe, where the penetration injury is at its most severe. We used voltammetry next to microdialysis probes to record electrically evoked DA release in the rat striatum during the retrodialysis of DXM and XJB-5-131 (XJB) over 4 hr.[25] Whereas DXM is an anti-inflammatory drug, XJB is an antioxidant targeted with high selectivity to the inner mitochondrial membrane, see Figure 1 for both these chemical structures.[51-53] We reasoned that XJB, a new investigative drug might effectively mitigate penetration injury, as injury is known to induce oxidative stress.[53] Studies have shown that XJB improves neurocognitive function in rats with a traumatic brain injury. We also reasoned that XJB might be particularly effective at protecting DA axons and terminals, which are reputed to be particularly sensitive to oxidative stress and mitochondrial dysfunction.[54, 55] Post mortem the brain tissue containing the probe track was examined by fluorescence microscopy using immunohistochemical markers for ischemia (fluorescent nanobeads), neuronal nuclei (Neu-N), blood born microglia (ED-1), and DA axons and terminals (tyrosine hydroxylase, TH).

Voltammetry measurements of DA concentrations were recorded a short distance away from the probe (70−100 μm). In the case of microdialysis probes perfused with unmodified artificial cerebrospinal fluid (aCSF) (i.e. no DXM, no XJB), implanting the microdialysis probe next to the voltammetric electrode abolished the electrically evoked DA response. Next, a single dose of nomifensine, a DA reuptake inhibitor well known to increase the concentration of DA observed during electrical stimulation procedures was administered.[26, 28] Stimulated DA release was observed following the dose of nomifensine (Fig. 12a, green). The response obtained after nomifensine (Fig. 11a, green) was interesting in that the DA signal was detected right away when the stimulus begin, roughly during the first 250 ms. In the rat striatum the reported diffusion coefficient of DA is 2.4×10^{-6} cm^2/s, thus the average diffusion distance in 250 ms is ~11 μm.[56] Therefore the DA detected early on in the stimulus was released from DA terminals which are in close proximity to the microelectrode. This extends a previous suggestion that DA terminals near the microdialysis probes are surviving but could be in a suppressed state.[57] This motivated our on-going efforts to preserve the activity of those surviving DA terminals.

When microdialysis probes were perfused with DXM, implanting the probe next to the microelectrode diminished electrically evoked DA release (Fig. 12b, red). The retrodialysis of DXM diminished the loss in amplitude of the DA response; this possibly indicates improved survival of DA terminals in the tissue near the probe. With the intent of comparing the results obtained using probes perfused with unmodified aCSF, we again recorded a stimulus response after treating the animals with nomifensine (Fig. 12b, green): DXM substantially improved the amplitude of the post-nomifensine response. The loss in the DA response amplitude was also diminished, both before and after administration of nomifensine in probes perfused with XJB (Fig. 12c). As in the case during aCSF perfusion; DA was rapidly detected at the start of the

stimulus after nomifensine administration, indicating the presence DA terminals surviving in close proximity to the voltammetric microelectrode. Collectively, these results confirm that both DXM and XJB preserved DA activity in the tissue next to the microdialysis probes.

Following *in vivo* measurements, the brain tissue containing the microdialysis probe tracks was examined by fluorescence microscopy using markers for ischemia, neuronal nuclei, macrophages, and DA axons and terminals (Fig. 13). As we reported before, probes perfused with unmodified aCSF caused profound ischemia (reduced blood flow), as indicated by a near-total absence of fluorescent nanobeads in the tissues surrounding the probe tracks.[38, 58] Both DXM and XJB increased the presence of nanobeads near the probe tracks, demonstrating in both cases a decrease in ischemia.

Decreased NeuN labeling was observed in tissue that was perfused with unmodified aCSF; this decrease indicates a loss of striatal neurons near the probes. An increase in ED-1 labeling was observed indicative of infiltration and activation of microglia near the probes in this same tissue. For the reason that the ED-1 marker specifically labels blood-derived microglia (i.e. macrophages) an opening of the blood-brain barrier is most likely.[59] Both DXM and XJB increased NeuN labeling and decreased ED-1 labeling, this signifies that both drugs protect the brain tissue near the probes.

TH labeling was punctate in striatal non-implanted tissue; TH labeling corresponds to the size and distribution of DA axons and terminals. When the probes were perfused with unmodified aCSF punctate labeling was eliminated, revealing profound disruptions of DA axons and terminals. The edges of the probe track had intense labeling; however, this was not punctate and reflects non-specific binding.[60] The loss of punctate TH labeling does not inevitably mean a loss of DA axons and terminals but rather that the axons and terminals have lost their TH.

Despite this, microscopy confirmed that the probes caused a profound disruption of DA axons and terminals. Punctate TH labeling was preserved using DXM and XJB. These immunohistochemical findings characterize the ability of DXM and XJB to preserve DA activity as assessed by voltammetry next to microdialysis probes (Fig. 13).

Our findings revealed that retrodialysis of DXM or XJB mitigates penetration injury during brain microdialysis. Striatal DA activity was protected using these two drugs as assessed by "voltammetry next to microdialysis probes." Histochemical changes in the tissues near the probes were mitigated with both drugs. The effects on DA activity correlated with the observed histochemical changes are potentially significant as new neuroprotection strategies are expanding rapidly in the field of neuroscience. [61-64]

4. Conclusion

In this review we have discussed some of the differences of the tissue that surrounds microdialysis probes and microelectrodes in conjugation with FSCV for monitoring DA in the central nervous system. Many of these differences are due to the penetration injury into living brain tissue. Not only does a gradient of DA exist throughout the traumatized tissue layer, we have also demonstrated that the BBB is compromised which in turn creates a FBR. Evidence strongly suggests that the FBR alters the tissue in the vicinity of the probes limiting the efficacy of microdialysis studies. We have achieved encouraging results using DXM and XJB in order to mitigate disruption of the tissue near the probes. Retrodialysis of DXM was especially successful as it stabilized evoked DA responses and was highly effective at preventing ischemia and inhibiting glial activation surrounding the microdialysis probes.

Despite the complexity of living systems and the problems associated with *in vivo* measurements using microdialysis probes, we have made progress in improving the overall

health of the tissue surrounding the probe. Understanding and mitigating some of the FBR to probe insertion in acute and chronic studies will have a long-lasting and significant impact on the field of neuroscience. Prospects for substantially improving the technology of microdialysis, for both clinical and basic research applications, by temporarily modulating tissue responses through established pharmaceutical interventions appears to be critical and promising. Intracranial microdialysis has been an advantageous technique and growing consensus suggests that it likely to be an influential and prominent technique in clinical settings. It is becoming increasingly clear that microdialysis probes and microelectrodes provide a wealth of neurochemical information and could potential advance our understanding the multifaceted system of communication between neurons in the living brain.

5. Acknowledgements

This work was supported by the National Institute of Health, grant numbers: DA 13661, NS 081744, MH 075989 and MH 63122. The authors would also like to thank Kathryn M. Nesbitt, Erika L. Varner and Elaine M. Robbins for their help and assistance.

Table 1: List of compounds detected by microdialysis and/or FSCV.

Dialysate[a]	Region
Acetylcholine[65]	Hippocampus, prefrontal cortex[65]
Adenosine (diphosphate, monophosphate, triphosphate)[66]	Dorsal spinal horn[65]
Aspartate[65]	Striatum [65]
ATP[65]	
Benzodiazepine[67]	
Bombesin[68]	
Calcitonin gene-related peptide[66]	
Cholecystokinin[66]	Anterior cingulated cortex[65]
Cholinergic[66]	
Corticotropin releasing hormone [66]	Anterior pituitary[65]
DA[65]	Striatum[65]
Dynorphin α and β[66]	
Dynorphin α 1–8[66]	Striatum[65]
Dynorphins[66]	Striatum[65]
Endomorphin 1 and 2[66]	Spinal cord[65]
Epinephrine[66]	
GABA[65]	
Galanin[66]	Spinal cord[65]
Glutamate	Striatum[65]
Glycine[65]	Striatum[65]
Growth hormone releasing hormone[66]	Hypothalamus[65]
Histamine[65]	
Leucine-enkephalin[66]	Striatum[65]
Methionine-enkephalin[66]	Striatum[65]
Neurokinin α and β[66]	CSF[65]
Neuromedin U[66]	
Neuropeptide[66]	
Neuropeptide tyrosine[66]	Ventral striatum[65]
Neuropeptide Y[66]	
Neurotensin 8-13[66]	Ventral striatum[65]
Nitric oxide[65]	Striatum[65]
Nociceptin/orphanin FQ[66]	Hippocampus/thalamus[65]
Norepinephrine[66]	Striatum[65]
Opioid[66]	
Oxytocin[66]	Basal forebrain, perifornical hypothalamus, and locus ceruleus[65]
Sertonin[65]	Striatum[65]
Somatostatin[66]	Striatum[65]
β-Endorphin[66]	
Substance P[66]	CSF[65]
Tachykinin[66]	
Thyrotropin releasing hormone[66]	
Vasopressin[66]	Anterior pituitary[65]
Vasoactive intestinal polypeptide	Cerebral cortex tissue[65]
α-Melanocyte-stimulating-hormone[66]	

[a]Compounds in **bold font** can be detected using FSCV.

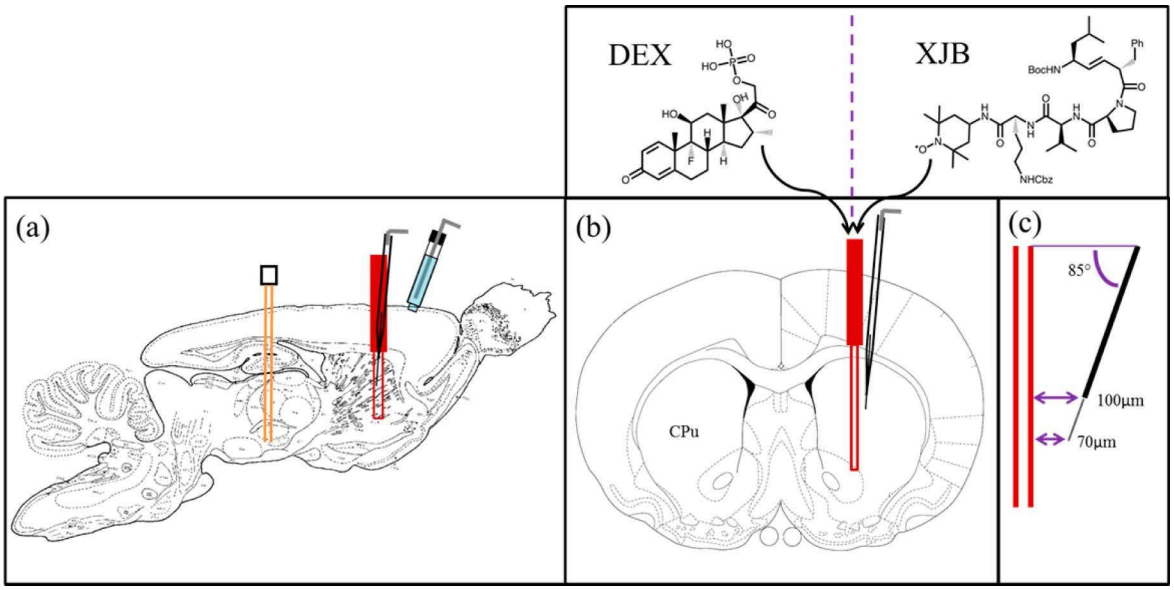

Fig. 1. Schematic of "voltammetry next to a microdialysis probe" in the rat brain. (a) A sagittal view of the stimulating electrode (orange) in the medial forebrain bundle, the microelectrode (black) and the microdialysis probe (red) in the striatum (CPu), and the Ag/AgCl reference electrode (blue) in contact with the brain surface. (b) A coronal view showing the microelectrode at a 5° angle from the probe. (c) The tip of the carbon fiber is 70 µm from the probe, and the top of the fiber is 100 µm from the probe. Drugs such as dexamethasone and XJB-5-131 are perfused through the probe. Reproduction reprint permission of *Anal. Chem.* © 2013.[25]

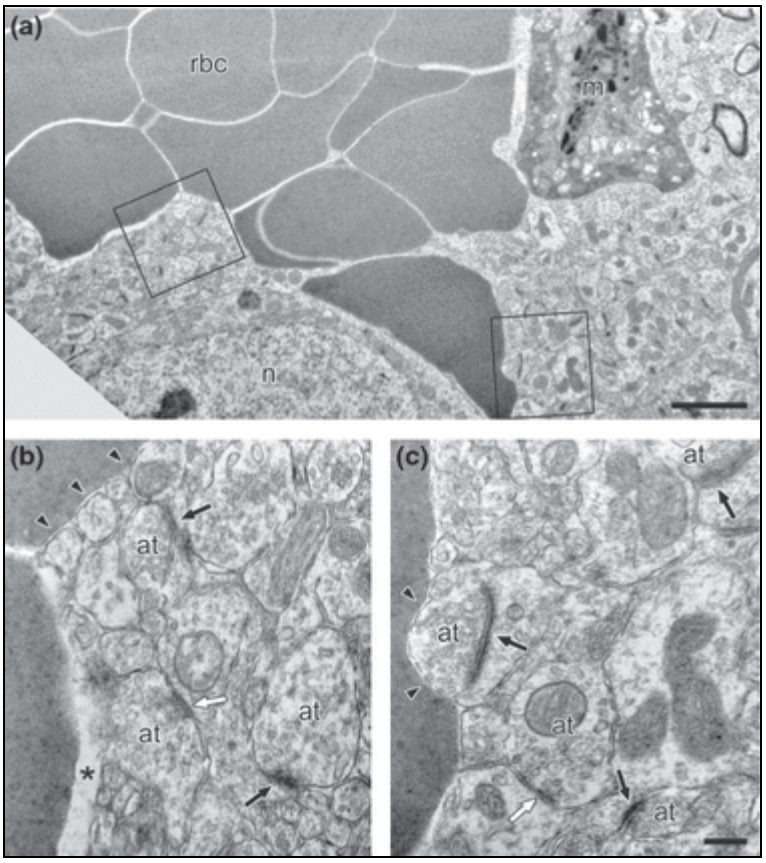

Fig. 2. Electron microscopic images of a carbon fiber track in the rat dorsal striatum. (a) At lower magnification, the track appears as an approximately round spot filled with red blood cells (rbc) that apparently fill the void formed when the electrode is explanted. Also visible are a single reactive monocyte (m) and the cell body of a neuron (n). The regions of interest outlined by boxes are shown at higher magnification in (b,c). Blood cells are directly apposed to neuronal structures (arrowheads) or separated from them by a slightly larger space (asterisk in b). The morphological appearance of these neuronal structures is normal. Multiple axon terminals (at) form symmetric (white arrows) or asymmetric synapses (black arrows) onto dendritic shafts or spines, respectively. Scale bar in (a) corresponds to 2 μm for (a) and the scale bar in (c) corresponds to 0.25 μm for (b) and (c). Reproduction reprint permission of *J. Neurochem* © 2012.[26]

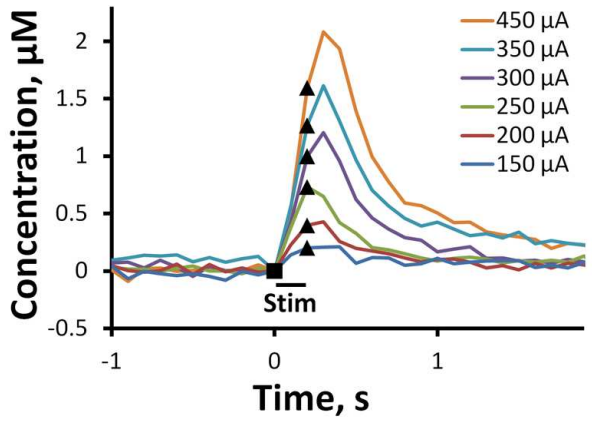

Fig. 3. Evoked DA responses with a carbon fiber microelectrode (200 µm long) recorded over a range of stimulus intensities ranging from 150 to 450 µA in the striatum of an anesthetized rat. Stimulation was delivered to the ipsilateral MFB at 60 Hz for 0.2s. The solid symbols mark the beginning (square) and ending (triangle) of each stimulus. Reproduction reprint permission of *ACS Chem. Neurosci.* © 2013.[27]

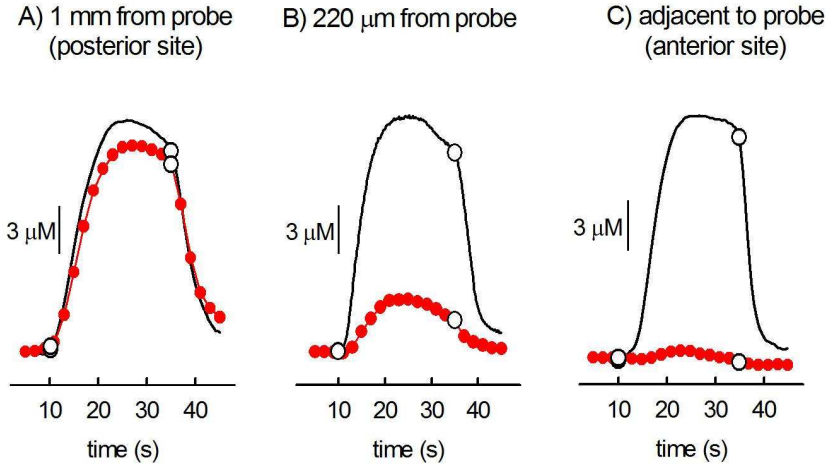

Fig. 4. Stimulus responses recorded in the striatum of an anesthetized rat with a voltammetric microelectrode at the posterior site (1 mm away from the probe) (A), 220µm away from the probe (B), and the anterior site (adjacent to the probe) (C). At each site, the solid line (black) is the voltammetric response before probe implantation and the dotted line (red) is the response 2 hrs after probe implantation. The open circles signify the start and end of the electrical stimulation. Reproduction reprint permission of *J. Neurosci. Methods* © 2005.[29]

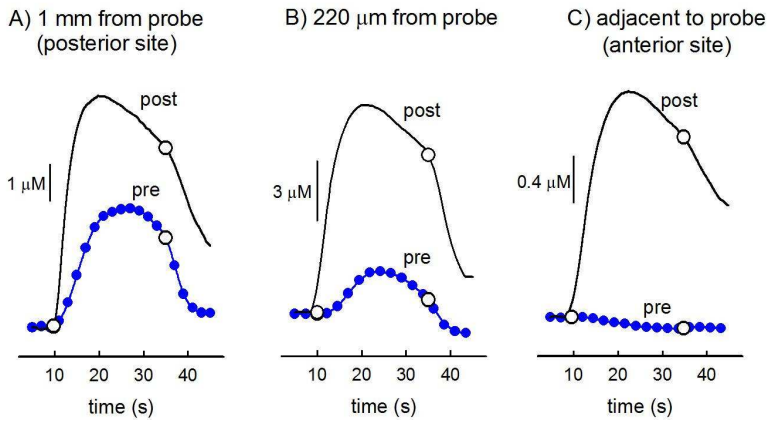

Fig. 5. Stimulus responses recorded in the striatum of an anesthetized rat with a voltammetric microelectrode before and after uptake inhibition. The experiment was initiated at least 2 hrs after probe implantation. Responses were recorded at sites 1 mm away from the probe (A), 220 μm from the probe (B) and adjacent to the probe (C). The responses were recorded before (pre, dotted line-blue) and 20-25 min after (post, solid line-black) systemic nomifensine (20 mg/kg i.p.). The open circles signify the start and end of the electrical stimulation. Reproduction reprint permission of *J. Neurosci. Methods* © 2005.[29]

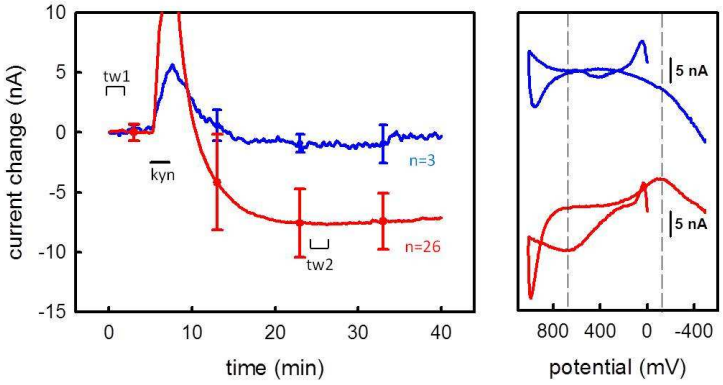

Fig. 6. Left panel: Intrastriatal microinfusion of kynurenate significantly decreases extracellular DA as measured by voltammetry in the striatum (red line) of an anesthetized rat. Microinfusion of kynurenate (kyn) into the parietal cortex had no prolonged effect on the voltammetric signal recorded at a nearby carbon fiber microelectrode (blue line). The horizontal bar labeled kyn indicates when the infusion took place. The lines were obtained by averaging the traces recorded in each of a group of animals (red, $\boldsymbol{n} = 26$ in 19 animals: blue, $\boldsymbol{n} = 3$ in 3 animals). The symbols indicate the mean and the standard deviations upon which statistical analyses were based. The infusion had a significant effect in the striatum (one-way ANOVA: $\boldsymbol{f} = 43.97$, d.f. = 3,103, $\boldsymbol{p} < 0.001$) but not in the parietal cortex. Right panel: Difference voltammograms obtained in the striatum (red line) and cortex (blue line). These difference voltammograms were obtained by subtracting the voltammograms recorded after the infusions (tw2, left panel) from those recorded before the infusion (tw1, left panel). The difference voltammogram obtained in the striatum exhibits DA oxidation and reduction features whereas that obtained in the cortex does not. Reproduction reprint permission of *J. Neurochem.* © 2004.[32]

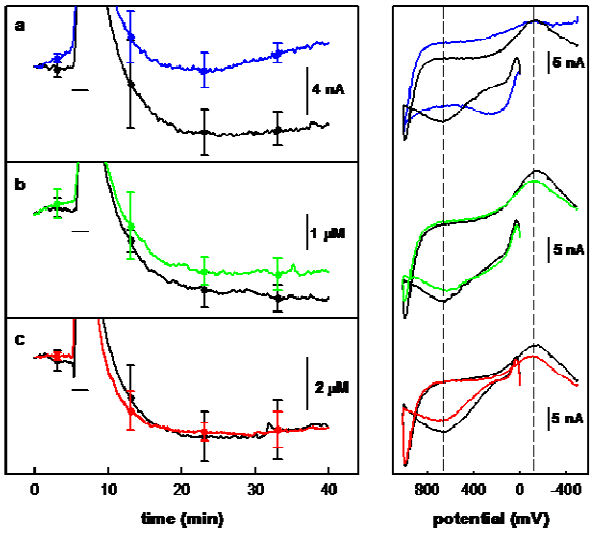

Fig. 7. Systemic administration of the nomifensine (20 mg/kg i.p.) either abolishes (a) or significantly diminishes (b) the effect of kynurenate on extracellular dopamine in the striatum of an anesthetized rat. (a) In four of eight animals (blue line), nomifensine eliminated the effect of kynurenate (two-way ANOVA; $p < 0.001$). In these animals, subtracted cyclic voltammograms obtained prior to nomifensine administration (black line) were characteristic of dopamine. Voltammograms obtained after nomifensine administration were not characteristic of dopamine (blue line). (b) In four other animals, systemic administration of nomifensine (green line) significantly diminished the response to kynurenate infusion (two-way ANOVA, $p < 0.05$). In the right panel; subtracted voltammograms were characteristic of dopamine both before (black line) and after (green line) nomifensine administration. (c) Systemic administration of saline had no affect on the response to kynurenate (two-way ANOVA). Voltammograms obtained before (black line) and after (red line) saline were characteristic of dopamine. The horizontal bars indicate when the infusions took place. Reproduction reprint permission of *J. Neurochem.* © 2004.[32]

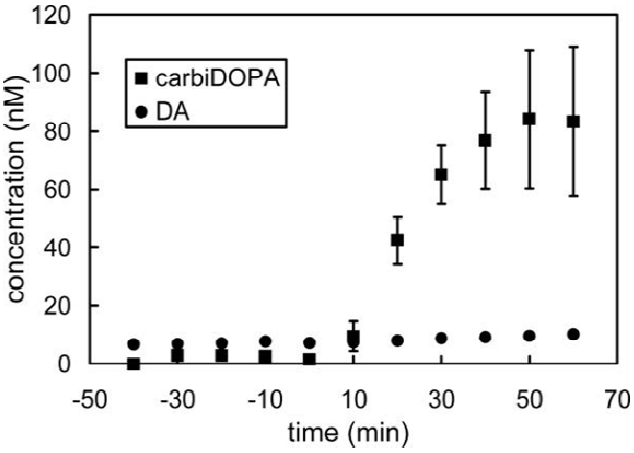

Fig. 8. Systemic administration of carbi-DOPA (150 mg/kg i.p.) 3 hours after probe implantation in an anesthetized rat. Microdialysis samples were collected from the striatum and concentrations of DA and carbi-Dopa were determined by high pressure liquid chromatography-photoluminescence following electron transfer detection. Administration of carbi-DOPA significantly increases dialysate carbi-DOPA levels (squares) but does not affect dialysate DA levels (circles). In the case of DA, the error bars are smaller than the symbols. Reproduction reprint permission of *J. Neurosci. Methods* © 2008.[37]

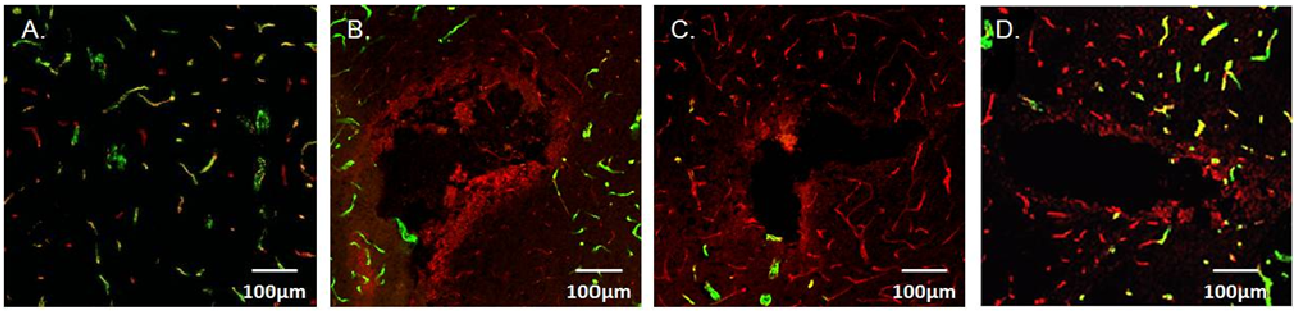

Fig. 9. Fluorescence microscopy of microdialysis probe *in vivo* of an anesthetized rat. Non-injured tissue (A) is compared to microdialysis probes tracks after 1 hr (B), 4 hr (C) and 24 hr (D) implants. Green (fluorescent beads) represents blood flow. Red represents blood vessels (anti-PECAM). In healthy tissue the red and green labeling overlay each other. Near the probe tracks the labels do not overlay, showing the presence of vessels (red) with no flow (no green). Moreover the red labeling is diffuse after acute microdialysis (Panel B), showing the release of the contents of endothelial cells into interstitial spaces. Over time, the diffuse labeling fades (Panels C and D), indicating that an active wound-healing process is underway. Scale bar represents 100µm. Reproduction reprint permission of *J. Neurosci. Methods* © 2009.[38]

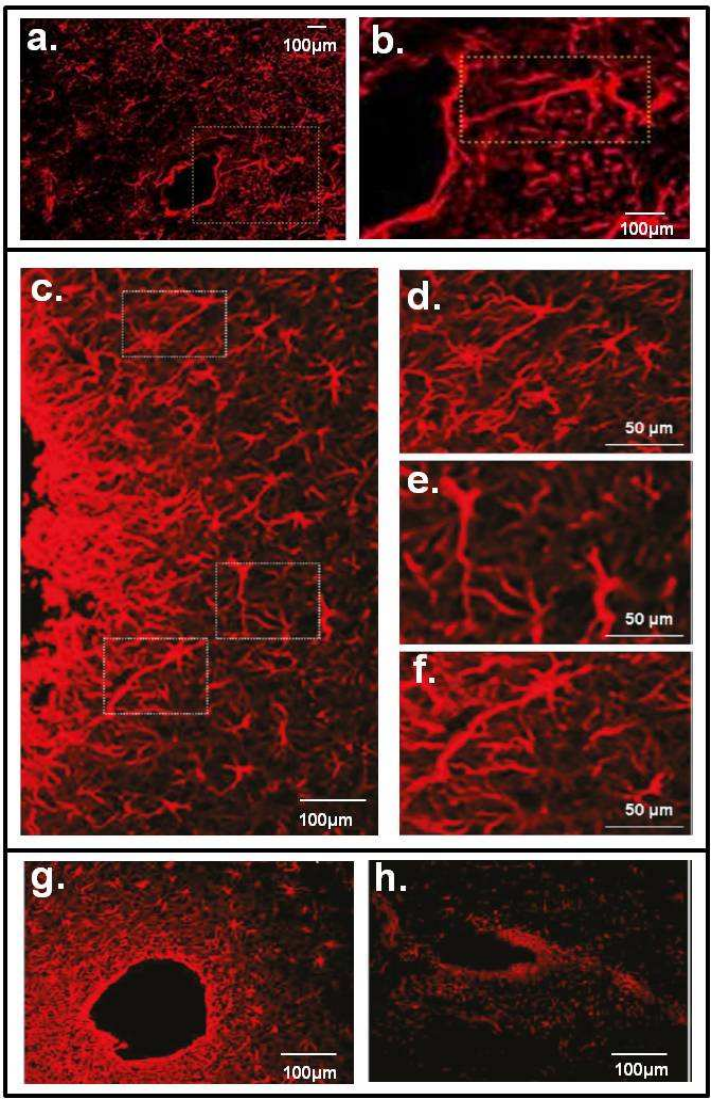

Fig. 10. Effect of *in vivo* microdialysis probes on striatal glial cells labeled with GFAP antibody of an anesthetized rat. a) A microdialysis probe track at 24 hours b) Enlargement of the area in the yellow box - shows a glial cell extending a process ~300 µm towards the track. Reproduction reprint permission of *J. Neurosci. Methods* © 2009. [38] c) Striatal tissue next to a microdialysis probe track at 5 days; the edge of the track is on the left side of the image. The right-hand column (panels d, e, and f) show enlargements of the white boxes in panel c. Reproduction reprint permission of *Anal. Chem*.© 2011.[49] g) GFAP image of a glial barrier formed after 5 days of microdialysis without DXM. h) GFAP image of a probe track after 5 days of retrodialysis of DXM. Reproduction reprint permission of *Anal. Chem*.© 2011.[49]

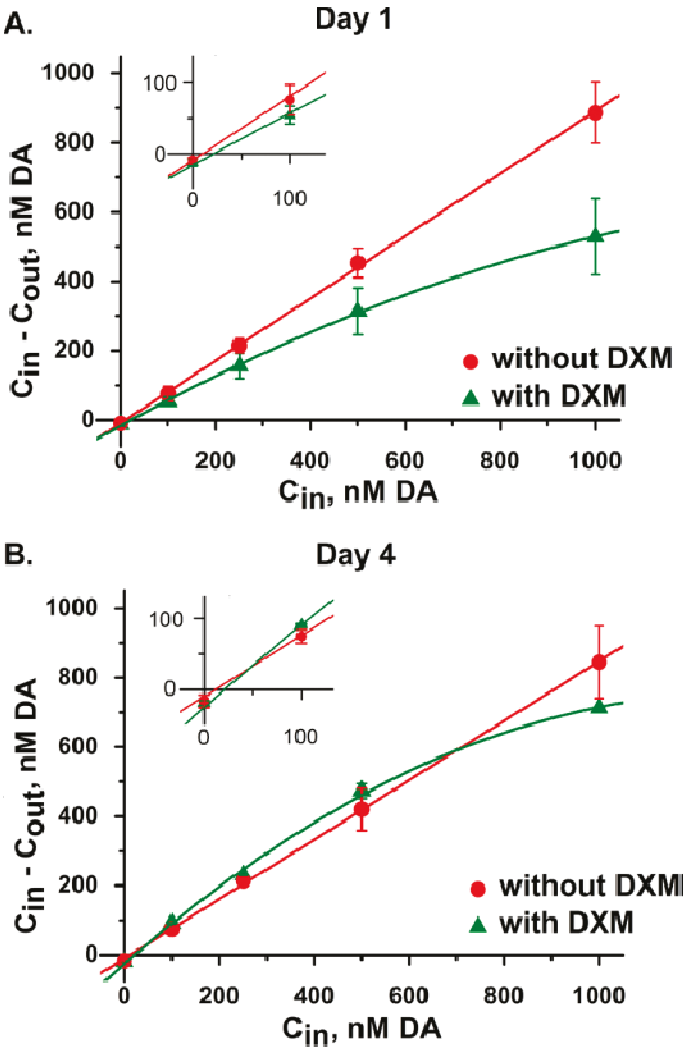

Fig. 11. DA concentration difference plots obtained in the rat striatum on day 1 (A) and day 4 (B) of microdialysis with (green) and without (red) DXM. The data points represent the mean ± (standard error). The solid lines show the linear regression of the data obtained without DXM (red) and the non-linear regression of the data obtained with DXM (green). Microdialysis probes (BASi MD-2204) were lowered over 30 minutes through the guide cannula into the striatum. The probes were perfused continuously for 5 days at 0.610 µL/min. Insets expand the region near the origin to visualize $C_{out,c}$ and C_{nnf}. Reproduction reprint permission of *Anal. Chem.*© 2011.[49]

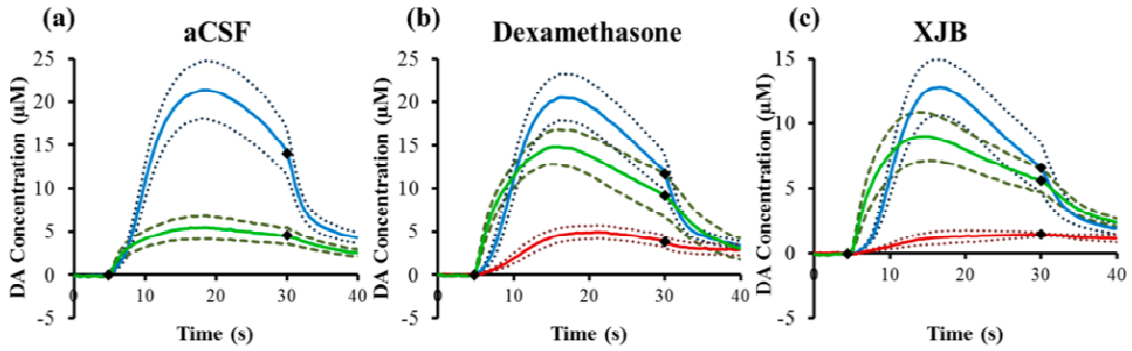

Fig. 12. Effect of aCSF (a), DXM (b), or XJB (c) on electrically evoked DA responses measured *in vivo* before implanting the probe (blue lines), 2 h and 40 min after implanting the probe (red lines, the response was non-detectable in a) and 25 min after nomifensine (green lines). The solid lines are the average of the responses in each group of rats (n = 6 per group), and the broken lines are confidence intervals based on the standard error of the mean of each data point. The black diamonds show when the stimulus begins and ends. Reproduction reprint permission of *Anal. Chem.* © 2013.[25]

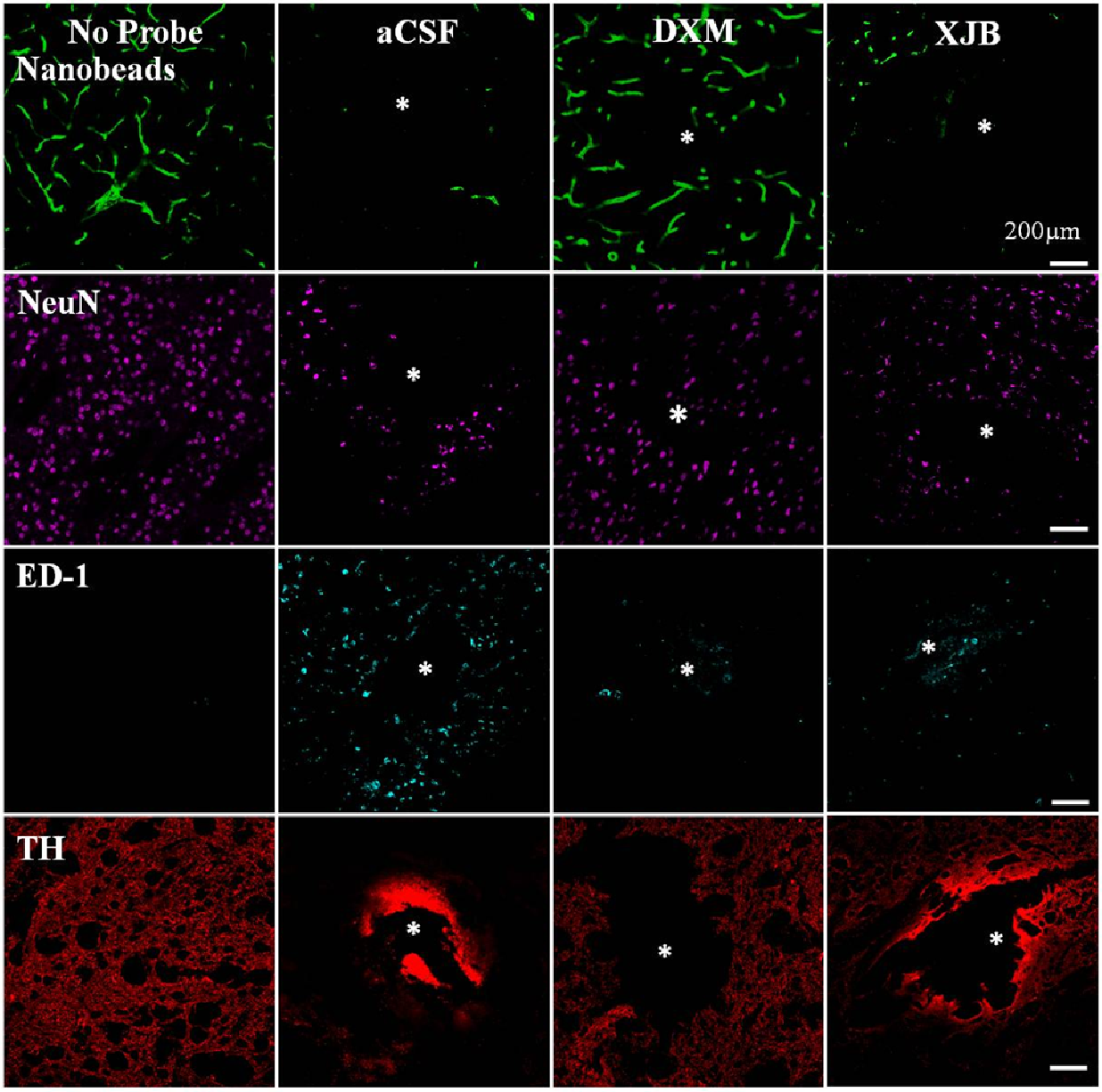

Fig. 13. DXM and XJB mitigate the histochemical impact of penetration injury in the striatum of an anesthetized rat. Separate columns provide representative images of tissue after retrodialysis of aCSF, DXM, and XJB for 4 h. The left-most column shows images of nonimplanted control striatal tissue. Separate rows provide representative images of tissue labeled with markers for blood flow (nanobeads), neuronal nuclei (NeuN), macrophages (ED-1), and DA axons and terminals (TH). The probe track is in the center of the images and marked with an asterisk. Scale bars are 200 μm. Reproduction reprint permission of *Anal. Chem*. © 2013.[25]

References

1. E. D. Abercrombie and M. J. Zigmond, *J Neurosci*, 1989, **9**, 4062-4067.
2. G. W. Arbuthnott, I. S. Fairbrother and S. P. Butcher, *J Neurosci Methods*, 1990, **34**, 73-81.
3. B. Bosche, C. Dohmen, R. Graf, M. Neveling, F. Staub, L. Kracht, J. Sobesky, F. G. Lehnhardt and W. D. Heiss, *Stroke*, 2003, **34**, 2908-2913.
4. G. Di Chiara, *J. Psychopharmacol.*, 1998, **12**, 54-67.
5. J. Kehr, in *Handbook of Behavioral Neuroscience*, eds. H. C. W. Ben and I. F. H. C. Thomas, Elsevier, 2006, vol. Volume 16, pp. 111-129.
6. U. Tossman, S. Eriksson, A. Delin, L. Hagenfeldt, D. Law and U. Ungerstedt, *J Neurochem*, 1983, **41**, 1046-1051.
7. U. Ungerstedt, in *In Measurement of Neurotransmitter Release In Vivo*, ed. C. A. Marsden, John Wiley & Sons, New York, 1984, pp. 81-105.
8. C. J. Watson, B. J. Venton and R. T. Kennedy, *Anal. Chem.*, 2006, **78**, 1391-1399.
9. B. H. Westerink and J. B. De Vries, *J. Neurochem.*, 1988, **51**, 683-687.
10. I. K. Wright, N. Upton and C. A. Marsden, *Psychopharmacology (Berl)*, 1992, **109**, 338-346.
11. T. Sharp, T. Zetterström, T. Ljungberg and U. Ungerstedt, *Brain Research*, 1987, **401**, 322-330.
12. A. Peters, L. S. Palay and H. deF. Webster, *The Fine Structure of the Nervous System*, W.B.Saunders Company, Philadelphia PA, 1976.
13. R. R. Holson, J. F. Bowyer, P. Clausing and B. Gough, *Brain Res*, 1996, **739**, 301-307.
14. R. R. Holson, R. A. Gazzara and B. Gough, *Brain Res*, 1998, **808**, 182-189.
15. T. E. Robinson and D. M. Camp, *J Neurosci Methods*, 1991, **40**, 211-222.
16. B. H. Westerink and M. H. Tuinte, *J Neurochem*, 1986, **46**, 181-185.
17. H. Yang and A. C. Michael, in *Electrochemical Methods for Neuroscience*, eds. A. C. Michael and L. M. Borland, CRC Press, Boca Raton (FL), 2007.
18. K. L. Clapp-Lilly, R. C. Roberts, L. K. Duffy, K. P. Irons, Y. Hu and K. L. Drew, *J. Neurosci. Methods*, 1999, **90**, 129-142.
19. F. Zhou, X. Zhu, R. J. Castellani, R. Stimmelmayr, G. Perry, M. A. Smith and K. L. Drew, *Am. J. Pathol.*, 2001, **158**, 2145-2151.
20. P. DeBoer and E. J. Abercrombie, *Pharmacol. Exp. Ther.*, 1996, **277**, 775-783.
21. M. Santiago and B. H. Westerink, *Naunyn-Schmiedebergs Arch. Pharmacol.*, 1990, **342**, 407-414.
22. E. C. de Lange, M. R. Bouw, J. W. Mandema, M. Danhof, A. G. de Boer and D. D. Breimer, *Br J Pharmacol*, 1995, **116**, 2538-2544.
23. O. Major, T. Shdanova, L. Duffek and Z. Nagy, *Acta. Neurochir.Suppl.*, 1990, **51**, 46-48.
24. E. C. M. de Lange, M. Danhof, A. G. de Boer and D. D. Breimer, *Brain Research Reviews*, 1997, **25**, 27-49.
25. K. M. Nesbitt, A. Jaquins-Gerstl, E. M. Skoda, P. Wipf and A. C. Michael, *Analytical Chemistry*, 2013, **85**, 8173-8179.
26. I. M. Taylor, A. Jaquins-Gerstl, S. R. Sesack and A. C. Michael, *J Neurochem*, 2012, **122**, 283-294.
27. I. M. Taylor, A. I. Ilitchev and A. C. Michael, *ACS Chemical Neuroscience*, 2013, **4**, 870-878.

28. P. A. Garris and R. M. Wightman, in *Neuromethods: voltammertic methods in brain systems*, eds. A. Boulton, G. Baker and R. N. Adams, Humana, Totowa, 1995, vol. 27, pp. 179-220.
29. L. M. Borland, G. Shi, H. Yang and A. C. Michael, *J. Neurosci. Methods*, 2005, **146**, 149-158.
30. H. Benveniste, J. Drejer, A. Schousboe and N. H. Diemer, *J.Neurochem.*, 1987, **49**, 729-734.
31. S. P. Butcher, J. Liptrot and G. W. Aburthnott, *Neuroscience Letters*, 1991, **122**, 245-248.
32. L. M. Borland and A. C. Michael, *Journal of Neurochemistry*, 2004, **91**, 220-229.
33. A. D. Smith and J. B. J. Justice, *J. Neurosci. Methods*, 1994, **54**, 75-82.
34. D. Sulzer, T. K. Chen, Y. Y. Lau, H. Kristensen, S. Rayport and A. Ewing, *J.Neurosci.*, 1995, **15**, 4102-4108.
35. J. D. Elsworth and R. H. Roth, *Exp Neurol*, 1997, **144**, 4-9.
36. T. D. Y. Kozai, A. S. Jaquins-Gerstl, A. L. Vazquez, A. C. Michael and X. T. Cui, *ACS Chemical Neuroscience*, 2015, **6**, 48-67.
37. C. M. Mitala, Y. Wang, L. M. Borland, M. Jung, S. Shand, S. Watkins, S. G. Weber and A. C. Michael, *J. Neurosci. Methods*, 2008, **174**, 177-185.
38. A. Jaquins-Gerstl and A. C. Michael, *J. Neurosci Methods*, 2009, **183**, 127-135.
39. T. Roitbak and E. Sykova, *Glia*, 1999, **28**, 40-48.
40. H. Benveniste and N. H. Diemer, *Acta. Neuropathol.*, 1987, **74**, 234-238.
41. S. K. L. Retterer S.T., Bjornsson C.S., Neeves K.B., Spence A.J.H., Turner J.N., Shain W., and Isaacson M.S. , *IEEE Transaction on Biomedical Engineering*, 2004, **51**, 2063-2073.
42. W. Shain, L. Spataro, J. Dilgen, K. Haverstick, S. Retterer, M. Isaacson, M. Saltsman and J. N. Turner, *IEEE Transaction on Neural Systems and Rehabilitation Engineering*, 2003, **11**, 186-188.
43. A. M. D. Szarowski D.H., Retterer S., Spence A.J., Isaacson M., Craighead H.G., Turner J.N., and Shain W, *Brain Res.*, 2003, **983**, 23-35.
44. Y. Zhong and R. V. Bellamkonda, *Brain Res.*, 2007, **1148**, 15-27.
45. B. H. C. Westerink, *J. Chromatogr. B.Biomed. Sci. Appl.*, 2000, **747**, 21-32.
46. L. Spataro, J. Dilgen, S. Retterer, A. J. Spence, M. Isaacson, J. N. Turner and W. Shain, *Exp. Neurol.*, 2005, **194**, 289-300.
47. Y. Zhong and R. V. Bellamkonda, *Journal of controlled release : official journal of the Controlled Release Society*, 2005, **106**, 309-318.
48. X. Mou, M. R. Lennartz, D. J. Loegering and J. A. Stenken, *Journal of diabetes science and technology*, 2011, **5**, 619-631.
49. A. Jaquins-Gerstl, Z. Shu, J. Zhang, Y. Liu, S. G. Weber and A. C. Michael, *Anal Chem*, 2011, **83**, 7662-7667.
50. T. L. Laabs, H. Wang, Y. Katagiri, T. MaCann, J. W. Fawcett and H. M. Geller, *J. Neurosci.*, 2007, **27**, 14494-14501.
51. M. P. Fink, C. A. Macias, J. Xiao, Y. Y. Tyurina, R. L. Delude, J. S. Greenberger, V. E. Kagan and P. Wipf, *Critical care medicine*, 2007, **35**, S461-467.
52. J. Jiang, I. Kurnikov, N. A. Belikova, J. Xiao, Q. Zhao, A. A. Amoscato, R. Braslau, A. Studer, M. P. Fink, J. S. Greenberger, P. Wipf and V. E. Kagan, *J Pharmacol Exp Ther*, 2007, **320**, 1050-1060.

53. P. Wipf, J. Xiao, J. Jiang, N. A. Belikova, V. A. Tyurin, M. P. Fink and V. E. Kagan, *Journal of the American Chemical Society*, 2005, **127**, 12460-12461.
54. R. L. Hunter, N. Dragicevic, K. Seifert, D. Y. Choi, M. Liu, H. C. Kim, W. A. Cass, P. G. Sullivan and G. Bing, *J Neurochem*, 2007, **100**, 1375-1386.
55. J. Ji, A. E. Kline, A. Amoscato, A. K. Samhan-Arias, L. J. Sparvero, V. A. Tyurin, Y. Y. Tyurina, B. Fink, M. D. Manole, A. M. Puccio, D. O. Okonkwo, J. P. Cheng, H. Alexander, R. S. Clark, P. M. Kochanek, P. Wipf, V. E. Kagan and H. Bayir, *Nat Neurosci*, 2012, **15**, 1407-1413.
56. C. Nicholson and M. E. Rice, in *Volume Transmission in the Brain*, eds. K. Fuxe and L. F. Agnati, Raven Press, New York, 1991, pp. 279–294.
57. Y. Wang and A. C. Michael, *J Neurosci Methods*, 2012, **208**, 34-39.
58. C. M. Mitala, Y. Wang, L. M. Borland, M. Jung, S. Shand, S. Watkins, S. G. Weber and A. C. Michael, *J Neurosci Methods*, 2008, **174**, 177-185.
59. L. Rinaman, J. P. Card and L. W. Enquist, *J Neurosci*, 1993, **13**, 685-702.
60. M. Sauer, J. Hofkens and J. Enderlein, *Handbook of Fluorescence Spectroscopy and Imaging: From Ensemble to Single Molecules*, WILEY-VCH verlag & Co., Germany, 2011.
61. N. Han, S. S. Rao, J. Johnson, K. S. Parikh, P. A. Bradley, J. J. Lannutti and J. O. Winter, *Frontiers in neuroengineering*, 2011, **4**, 2.
62. T. W. Hsiao, V. P. Swarup, B. Kuberan, P. A. Tresco and V. Hlady, *Acta biomaterialia*, 2013.
63. L. Karumbaiah, S. E. Norman, N. B. Rajan, S. Anand, T. Saxena, M. Betancur, R. Patkar and R. V. Bellamkonda, *Biomaterials*, 2012, **33**, 5983-5996.
64. D. Y. Lewitus, K. L. Smith, W. Shain, D. Bolikal and J. Kohn, *Biomaterials*, 2011, **32**, 5543-5550.
65. J. W. Kebabain and Neumeyer, J.L., *RBI Handbook of Receptor Classification*, 1994.
66. M. Perry, Q. Li and R. T. Kennedy, *Anal. Chim. Acta.*, 2009, **653**, 1-22.
67. C. W. Bradberry, J. D. Lory and R. H. Roth, *Journal of Neurochemistry*, 1991, **56**, 748-752.
68. D. S. Michaud, J. McLean, S. E. Keith, C. Ferrarotto, S. Hayley, S. A. Khan, H. Anisman and Z. Merali, *Neuropsychopharmacology*, 2003, **28**, 1068-1081.

TOC

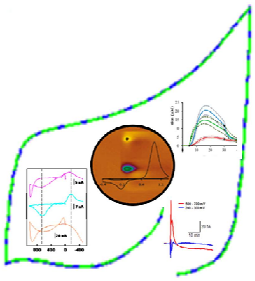

We review the work of “voltammetry next to a microdialysis probe” as measured by dopamine and the surrounding tissue.